HDV Ribozyme Activity in Monovalent Cations†

Anne T. Perrotta and Michael D. Been*

Department of Biochemistry, Box 3711, Duke University Medical Center, Durham, North Carolina 27710

Received June 19, 2006; Revised Manuscript Received July 29, 2006

ABSTRACT: Activity of the two ribozymes from hepatitis delta virus in monovalent salts was examined and compared to activity in Mg^{2+}. Both ribozymes self-cleaved in high concentrations of monovalent cations, and an active site cytosine was required for cleavage activity under those conditions. Cleavage rates were 30−50-fold higher for reactions in LiCl than for reactions in NaCl or NH_4Cl, and a thio effect indicated that chemistry was rate-determining for cleavage of the HDV genomic ribozyme in LiCl. Still, in LiCl, there was a more than 100-fold increase in the rate when $MgCl_2$ was included in the reaction. However, the pH−rate profiles for the reactions in LiCl with and without $MgCl_2$ were both bell-shaped with the pH optima in the neutral range. These findings support the idea that monovalent cations can partially substitute for divalent metal ions in the HDV ribozymes, although a divalent metal ion is more effective in supporting catalysis. The absence of a dramatic change in the general shape of pH−rate profiles in LiCl, relative to the profile for reactions including Mg^{2+}, is in contrast to earlier data for the reactions in NaCl and limits our interpretation of the specific role played by the divalent metal ion in the catalytic mechanism.

The hepatitis delta virus (HDV)[1] ribozymes are small self-cleaving RNAs which, like the hammerhead, hairpin, and *Neurospora* VS ribozymes, are a feature of some small RNA replicons where they are thought to process rolling-circle replication products to monomer sizes (*1*, *2*). These small ribozymes catalyze RNA backbone cleavage via a group transfer or exchange reaction in which the 3′,5′-phosphodiester bond is rearranged to generate a 2′,3′-cyclic phosphate group and a 5′-hydroxyl group at the break (*3*). Those products suggest that the 2′-hydroxyl group adjacent to the cleavage site phosphate group is the nucleophile in a backbone cleavage reaction. This is a common reaction involving RNA, yet our understanding of the mechanism of catalysis in ribozyme self-cleavage remains incomplete. In the HDV ribozymes, there is a cytosine nucleobase located in the active site pocket (*4*−*6*) that appears to act as a general acid−base catalyst (*7*−*11*). Recent data support a model in which the role of the cytosine is to donate a proton to the leaving group (5′) oxygen (*12*). A more complete version of a model for the catalytic mechanism has a divalent metal ion-bound hydroxide ion accept a proton from the 2′-oxygen nucleophile (*7*, *13*). The two groups could act in concert such that there is partial proton transfer at both positions in the transition state. Evidence for a divalent metal ion in the active site of a precursor form of the genomic HDV ribozyme has recently been observed, but it did not necessarily appear to be in position to function as a general base catalyst in that structure (*6*).

When salt conditions are near physiological, many of the small self-cleaving ribozymes are most active in the presence of low millimolar concentrations of divalent metal ions. Nevertheless, appreciable levels of cleavage activity are detected in the absence of divalent metal ions under a variety of conditions (*7*, *13*−*18*). The hairpin ribozyme in particular is highly active in high concentrations of monovalent metal ion or lower concentrations of spermidine or cobalt(III)−hexammine complex $[Co^{3+}(NH_3)_6]$, in the absence of Mg^{2+} (*14*−*16*). More recently, it has also been shown that the glmS ribozyme is active in $Co^{3+}(NH_3)_6$ (*19*). Activity in $Co^{3+}(NH_3)_6$ is evidence that the mechanism of catalysis requires neither the direct involvement of a metal-bound water nor inner-sphere coordination of a multivalent metal ion to the RNA. Although not active in $Co^{3+}(NH_3)_6$, the hammerhead ribozyme was active in the absence of divalent metal ions when high concentrations (1−4 M) of monovalent metal ion were present (*17*, *20*, *21*). However, it was ∼10−100-fold less active under those conditions than with divalent metal ions. That difference in activity suggests that there could be a unique contribution of divalent metal ion to catalysis with the hammerhead ribozyme, but it is difficult to pinpoint an exact role from those kinetic studies (*20*−*22*).

The two HDV ribozymes (Figure 1) are active in a variety of divalent metal ions, including Mg^{2+}, Ca^{2+}, and Mn^{2+}, but cleavage does not occur in $Co^{3+}(NH_3)_6$ (*6*, *13*, *23*). While activity with $Co^{3+}(NH_3)_6$ can be evidence that a divalent metal ion is not required in some roles as a catalyst (for example, as a general acid−base catalyst or directly coordinated to the nucleophilic oxygen), lack of activity, or inhibition by $Co^{3+}(NH_3)_6$, is not necessarily evidence that a divalent metal ion is required as a catalyst in those same roles. However, cleavage activity in the absence of divalent metal ion was detected in 1 M NaCl (*7*, *13*, *18*). While the

† Supported by National Institutes of Health Grant GM047233.

* To whom correspondence should be addressed. E-mail: mdbeen@duke.edu. Telephone: (919) 684-2858. Fax: (919) 684-5040.

[1] Abbreviations: HDV, hepatitis delta virus; EDTA, (ethylenedinitrilo)tetraacetic acid; Tris, tris(hydroxymethyl)aminomethane; MES, 2-(*N*-morpholino)ethanesulfonic acid.

10.1021/bi061215+ CCC: $33.50
Published on Web 08/29/2006

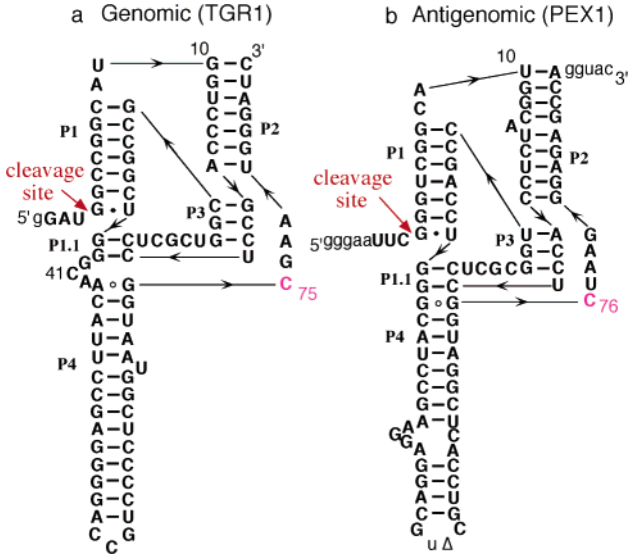

FIGURE 1: Sequence and secondary structures of the HDV genomic and antigenomic ribozymes used in this study. The complete sequence of the runoff transcript is shown. Lowercase letters denote differences from wild-type sequences: (a) genomic form of the ribozyme, TGR1, and (b) antigenomic form of the ribozyme, PEX1.

rates of cleavage were substantially lower than that with the divalent metal ion, the reaction in monovalent salts offered an additional approach to defining the metal ion requirements and roles in these two ribozymes. Previous studies in the Bevilacqua lab reveal that the HDV genomic ribozyme cleaved ~10^3-fold more slowly in 1 M NaCl than in 10 mM $MgCl_2$ (*7*). We saw comparable activity using a genomic ribozyme but found that under similar conditions (1 M NaCl) cleavage activity of an antigenomic ribozyme sequence was even slower (*18*). The difference in the behavior of the two HDV ribozymes in the absence of added Mg^{2+} was thought to reflect different features of the two ribozymes under those particular conditions but not a fundamental difference in the catalytic mechanism (*18*). In agreement with that idea, we show here that, in the absence of added Mg^{2+}, the antigenomic ribozyme is nearly as active as the genomic form when the monovalent salt concentration was increased above 1 M.

The comparison of activity of the HDV genomic ribozyme in Na^+ and Mg^{2+} as a function of pH has also provided evidence that has been interpreted as support for a model in which the conjugate base of a hydrated Mg^{2+} acts as a general base catalyst in the cleavage reaction (*7*, *13*). In those studies, dramatic changes in the shape of the pH−rate profiles were observed as metal ions and pH are varied. The switch from a pH−rate profile that followed a rate law definition of general base catalysis to one that followed general acid catalysis when Mg^{2+} was omitted appeared to be consistent with a role for a hydrated Mg^{2+} as a general acid−base catalyst. In the proposed mechanism, the $Mg(OH)^+$ acts as a general base catalyst and accepts the proton from the 2′-OH group as it attacks the phosphorus of the scissile phosphate (*7*). We had questioned that explanation of the "general acid"-shaped pH−rate profile (*18*), although the model for catalysis remains attractive.

Here we have examined the activity of the HDV ribozymes in several monovalent cations. Both ribozymes were more active in LiCl than in the other monovalent salts that were tested, and the effect of introducing a thiophosphate at the cleavage site suggested that chemistry could be rate-limiting for the reactions in LiCl. Nevertheless, the cleavage rates for the wild-type ribozymes were still much slower in LiCl than in $MgCl_2$. Despite a large decrease in the rate of the reaction, the shape of the pH−rate profile in LiCl was not dramatically different from that observed for the reactions in $MgCl_2$. The data are consistent with a catalytic role for Mg^{2+} but do not distinguish between it participating as a general acid−base catalyst and other involvement, such as direct coordination to the nucleophilic or leaving group oxygen, or perhaps as an electrostatic catalyst.

MATERIALS AND METHODS

Ribozymes and General Methods. The two HDV ribozymes used in this study are similar in size and were prepared and labeled with ^{32}P during transcription from cut plasmid DNA with T7 RNA polymerase as previously described (*24*, *25*). The genomic (TGR1) (Figure 1a) contained four nucleotides 5′ to the cleavage site and 85 nucleotides 3′ to the cleavage site. The antigenomic form (PEX1) (Figure 1b) contained eight nucleotides 5′ to the cleavage site and 93 nucleotides 3′ to the cleavage site. The sequences forming the core region or active site (*4*) of both ribozymes used in this study are wild-type sequence. Prior to the cleavage reactions, the RNAs were subjected to brief heating at 95 °C for 2 min and then preincubated in 5 mM Tris-HCl, 0.5 mM spermidine (or 100 mM NaCl), and 1 mM EDTA at neutral pH and 37 °C for 10 min. A prewarmed (37 °C), buffered monovalent salt solution was added to start the reaction; the final reaction mixture contained ≥25 mM EDTA and the salt as specified in the experiment. A three-buffer system {25 mM acetic acid, 25 mM MES [2-(*N*-morpholino)ethanesulfonic acid], and 50 mM Tris (pH 4.0−8.0) or 50 mM MES, 25 mM Tris, and 25 mM AMP (2-amino-2-methyl-1-propanol) (pH 7.0−10.0)} (*26*) was used, and the pH values at specific salt concentrations were measured in mock reaction mixtures containing all components except RNA. The cleavage reaction mixtures in monovalent cations were at 37 °C, unless otherwise specified. Reactions were terminated by dilution with 2 volumes of formamide containing 50 mM EDTA and freezing on powdered dry ice. Collected samples were thawed and immediately fractionated on polyacrylamide gels under denaturing conditions. The fraction cleaved (*f*) for each time point (*t*) was quantified from the dried gel using a Phosphorimager (Molecular Dynamics). Those data were fit (KaleidaGraph, Synergy Software) to the first-order rate equation $f = F(1 - e^{-k_{obs}t})$, where *F* is the end point fraction cleaved and k_{obs} is the apparent first-order rate constant. Under conditions where cleavage activity could be followed to near completion, the ribozymes cleaved with first-order kinetics and gave end points of 70−90% cleavage. End points varied in that range with the different ribozymes and salt conditions. To estimate rate constants for particularly slow reactions, an end point of 0.8 was used for nonlinear curve fitting, or the slope from a linear fit to the first 5−20% of the reaction was used. Determining the rate constants for cleavage reactions in Mg^{2+} without monovalent salt was similar except the dry ice freezing step was unnecessary (*18*, *27*).

pH Measurements. All reaction pH values were measured in mock reaction cocktails without the RNA. Several available glass combo electrodes were compared, and all gave similar pH readings in the high-salt buffers. To estimate the effect that monovalent salts had on pH reading, the pH of 10^{-2} nd 10^{-3} M HCl with and without 4 M LiCl was measured. The addition of 4 M LiCl caused the pH to read lower by 0.93 ± 0.06 in 10^{-2} and 10^{-3} M HCl. In 10^{-3} and 10^{-2} M NaOH, the LiCl caused a shift to a lower reading by 1.7 ± 0.1 and 1.9 ± 0.1 pH units, respectively. We concluded, by crude extrapolation to neutral pH, that the LiCl and other salts may lower pH readings as much as 1.4 pH units in the neutral range. However, the pH values given throughout the text and figures have not been adjusted for this value.

Thiophosphate-Containing Ribozymes. PEX1.2, PEX1.2S, TGR1.2, and TGR1.2(S) are self-cleaving forms of the antigenomic and genomic ribozymes prepared by ligation of a short chemically synthesized oligoribonucleotide, containing either a phosphate or a thiophosphate (the mixed diastereoisomer of a nonbridging oxygen to sulfur substitution) at the cleavage site, to a shortened form of the respective ribozymes using the method of Moore and Sharp (*28*). The 3′ portion of the ribozyme was prepared by transcription of a template in which the first nucleotide was G8 in the antigenomic or G6 in the genomic form of the ribozyme sequence (*29*). Transcription conditions included, in addition to the four NTPs at 1 mM each, GMP at 10 mM, and the $MgCl_2$ concentration was increased to 25 mM. Gel-purified 3′ ribozyme RNA (125 pmol) was annealed with the 5′ RNA oligonucleotide and a complementary DNA "splint" (625 pmol each) in a 20 μL reaction mixture by heating to 95 °C followed by slow cooling to room temperature and then ligated with DNA ligase overnight at room temperature in a buffer containing 66 mM Tris-HCl (pH 7.6), 6.6 mM $MgCl_2$, 1 mM DTT, 66 mM ATP, and 28% glycerol. Following ligation, the RNAs were fractionated by gel electrophoresis and the precursor form was isolated. The oligonucleotides were purchased from Dharmacon. The sequences of the oligonucleotides were 5′-UUC*GGGUCGG-3′ (antigenomic) and 5′-GGAU*GGCCG-3′ (genomic), where the asterisk marks the position of the thiophosphate substitution (the cleavage site). The oligodeoxynucleotide splint was 21 nucleotides long and spanned the ligation site.

RESULTS

Genomic HDV Ribozyme Activity in the Absence of Divalent Metal Ions. In the absence of added divalent metal ions, the self-cleavage activity of the genomic ribozyme (TGR1) was supported by high concentrations of a monovalent cation (Na^+, Li^+, or NH_4^+). The rate constant for cleavage increased with salt concentrations up to 2−5 M, depending on the salt (Figure 2 and Table 1). Evidence for possible saturation was most apparent in NaCl where the concentration−rate profile leveled off above 2 M (Figure 2a). When Na^+ was replaced with Li^+, the rate constant for the self-cleavage reaction increased by 30−50-fold in the concentration range that was tested (Figure 2b and Table 1). Activity was also found in NH_4Cl (Figure 2c), and the cleavage rate was ∼2-fold higher than in NaCl (Table 1). Much lower rates were measured in KCl and CsCl.

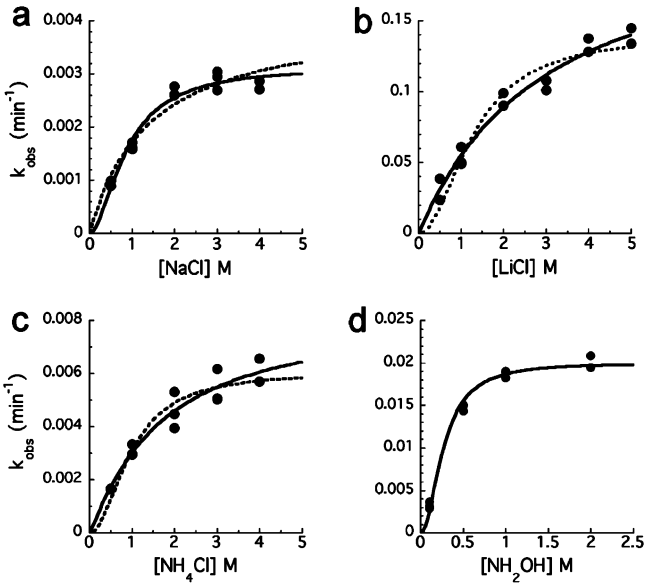

FIGURE 2: Cleavage rates of the genomic ribozyme (TGR1) increased with increasing concentrations of monovalent salts. Observed rate constants (k_{obs}) were determined in NaCl (pH 6.1) (a), LiCl (pH 6.3) (b), NH_4Cl (pH 6.6) (c), and NH_3OH (pH 5.8) (d). The curves (—) were generated by fitting the data to a simple binding model where $k_{obs} = k_{max}[[M]^n/([M]^n + K_{D,app})]$, where [M] is the concentration of cation, $K_{D,app}$ is an apparent dissociation constant, and n is the Hill coefficient. The dashed lines were generated by fixing n to 1 (a) or 2 (b and c).

Table 1: Cleavage Rate Constants for the HDV Genomic and Antigenomic Ribozymes in Various Salts at 37 °C

	k_{obs} (min^{-1})[a]	
	TGR1 (genomic)	PEX1 (antigenomic)
4 M LiCl (pH 6.3)	$(1.3 \pm 0.1) \times 10^{-1}$	$(6.2 \pm 0.5) \times 10^{-2}$
4 M NaCl (pH 6.1)	$(3.6 \pm 0.4) \times 10^{-3}$	$(1.8 \pm 0.1) \times 10^{-3}$
2 M KCl (pH 6.4)	$(1.5 \pm 0.1) \times 10^{-3}$	
4 M CsCl (pH 6.6)	$(6.8 \pm 0.8) \times 10^{-4}$	
4 M NH_4Cl (pH 6.6)	$(6.7 \pm 0.4) \times 10^{-3}$	
0.2 M NH_2OH (pH 6.2)	$(1.1 \pm 0.1) \times 10^{-2}$	
0.2 M NH_4Cl (pH 6.2)	$(1.3 \pm 0.2) \times 10^{-3}$	
0.1 M NH_4Cl and 0.1 M NH_2OH (pH 6.2)	$(2.0 \pm 0.2) \times 10^{-3}$	
0.1 M NH_2OH (pH 5.8)	$(3.2 \pm 0.3) \times 10^{-3}$	
10 mM $MgCl_2$ (pH 7.5)[b]	26 ± 3	14 ± 1 (at 25 °C)

[a] The rate constants reported for KCl and CsCl are the average of two determinations; all others are the average of three or more determinations. [b] Reaction rates in 10 mM $MgCl_2$ for TGR1 are from ref *18*; those of PEX1 were determined on a rapid quench instrument at 25 °C.

Other small differences in cleavage activity were seen with the various cations. Fitting the concentration−rate data to binding curves generated Hill coefficients (n) between 2 and 1 depending on the salt. The Hill coefficients derived from curve fitting (solid lines, Figure 2) were 1.8 ± 0.3 for Na^+, 1.0 ± 0.3 for Li^+, 1.1 ± 0.4 for NH_4^+, and 1.6 ± 0.1 for NH_3OH^+. Curves with Hill coefficients fixed at 1 for the NaCl data or 2 for the LiCl and NH_4Cl data (Figure 2a−c, dashed lines) are shown for comparison. The salt concentrations at half-maximal cleavage rates were estimated to be 1.4 ± 0.3 M for NaCl, 2.1 ± 0.5 M for NH_4Cl, and 3.2 ± 0.6 M for LiCl. The appearance of cooperativity with the NaCl data suggests that there are at least two classes of monovalent cation ion binding sites in the ribozyme.

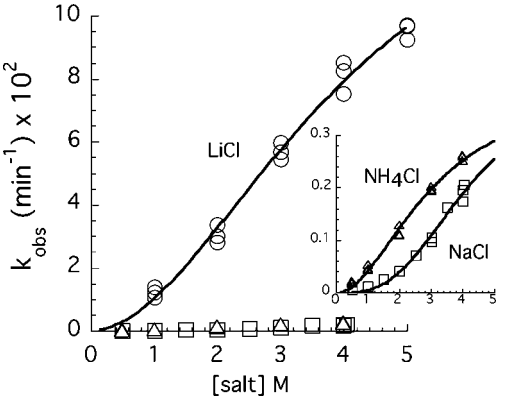

FIGURE 3: Cleavage rates of the antigenomic ribozyme (PEX1) increased with increasing concentrations of monovalent salts. Observed rate constants were determined in increasing concentrations of LiCl (○), NH_4Cl (△), or NaCl (□). The inset is a replot of the data for NH_4Cl and NaCl. Curves were generated as described in the legend of Figure 2. The Hill coefficients (n) were 1.9 ± 0.2, 1.9 ± 0.1, and 3.0 ± 0.2 for the reaction in LiCl, NH_4Cl, and NaCl, respectively.

Activity of the Antigenomic Ribozyme in Monovalent Salts. Previously, we had found that activity of a HDV antigenomic ribozyme (PEX1) in 1 M NaCl, with no added Mg^{2+}, was 10−20-fold lower than that of the genomic ribozyme under the same conditions (*18*). However, with higher concentrations of monovalent salts, those differences decreased. In 4 M LiCl, the antigenomic form of the HDV ribozyme cleaved nearly as fast as the genomic form (0.062 and 0.13 min^{-1}, respectively) (Figure 3 and Table 1). Likewise, in 4 M NaCl, the rate of cleavage of the antigenomic ribozyme approached that of the genomic form in NaCl (Table 1 and Figure 3, inset). As with the genomic ribozyme, NaCl was less effective than LiCl at supporting activity, and again cleavage in NH_4^+ was slightly faster than in Na^+. It was not possible to reach saturating conditions in these reactions, and it appears, in general, that the antigenomic ribozyme required higher concentrations of salt or cation to attain rates of cleavage comparable to those of the genomic ribozyme. Also, the curves are distinctly more sigmoidal than those of the genomic ribozyme, suggesting multiple classes of cation binding sites and cooperative cation binding.

Monovalent Salt Inhibition of Divalent Metal Ion-Dependent Activity. Cleavage rates of the ribozymes in $MgCl_2$ decreased with the addition of LiCl [Figure 4 (○)]. For the genomic ribozyme reaction in 2 mM $MgCl_2$ and 1 mM EDTA at 25 °C and pH 7, the apparent K_i of LiCl was 0.32 ± 0.04 M. However, inhibition appeared to be partial in that the rate constants at high LiCl concentrations with 1 mM Mg^{2+} (2 mM $MgCl_2$ and 1 mM EDTA) were always greater than rate constants for the reaction in the monovalent salt alone. In 1 mM Mg^{2+}, the rate constants leveled off at 1−2 min^{-1} with the higher LiCl concentrations. That was 10−20-fold faster than rates in just LiCl at pH 7. In 1, 2, and 3 M LiCl, increasing concentrations of $MgCl_2$ restored higher rates of cleavage (Figure 4, inset) which is consistent with competition for a metal ion binding site. Thus, LiCl supported cleavage activity and behaved as a partial competitive inhibitor in the faster Mg^{2+}-dependent reaction; the apparent K_d for Mg^{2+} increased with an increasing LiCl concentration, but with a higher $MgCl_2$ concentration, the cleavage rate constants for the ribozyme·Mg^{2+} and ribozyme·Li^+·Mg^{2+} complexes were similar. These results suggest multiple metal ion binding sites on the ribozyme, with at least one Mg^{2+}-occupied site conferring the higher rate of cleavage. Similar results are seen with both NaCl [Figure 4 (△)] and NH_4Cl (not shown). Also, the monovalent salts inhibited Mg^{2+}-dependent cleavage of the antigenomic ribozyme in much the same fashion (data not shown).

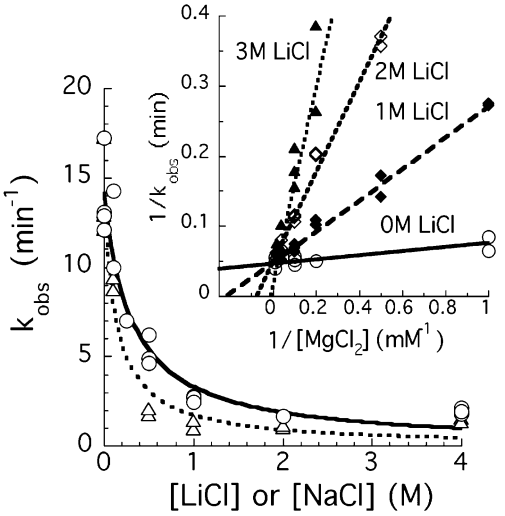

FIGURE 4: Mg^{2+}-dependent cleavage is inhibited by monovalent salts. Cleavage of the genomic ribozyme (TGR1) in 2 mM $MgCl_2$ and 1 mM EDTA with increasing concentrations of LiCl (○) or NaCl (△). The solid line shows a fit to the equation $k_{obs} = k_{Mg}/(1 + [LiCl]/K_{I,app})$, where $k_{Mg} = 14 \pm 1$ min^{-1} and $K_{I,app} = 0.32 \pm 0.04$ M. The dotted line is a visual aid for the NaCl data. The inset is a double-reciprocal plot of the $MgCl_2$ concentration dependence of the cleavage rate constants vs increasing LiCl concentrations. The concentrations of LiCl were 0 (○), 1 (◆), 2 (◇), and 3 M (▲).

The pH−Rate Profiles in Monovalent Salts Are Bell-Shaped. Bell-shaped pH−rate curves are characteristic of self-cleavage kinetics of the HDV genomic ribozyme, TGR1, in $MgCl_2$ (*18*) [Figure 5a (◇)]. The pH−rate profiles in LiCl, NaCl, and NH_4Cl [Figure 5b (●, ■, and ▲, respectively)] are also bell-shaped, but the curves are somewhat broader and the pH optima lower than those observed in Mg^{2+} (pH ∼6−7 compared to pH 7.5; Figure 5b). A broadening of the pH−rate curves in the absence of Mg^{2+} could be due to a change in the ionization constants of catalytic groups or the introduction of a pH-independent rate-determining step. In an earlier study, a pH−rate profile for a HDV genomic ribozyme cleavage in 1 M NaCl and 1 mM EDTA exhibited the highest activity below pH ∼6 and decreased as the pH increased; thus, it followed the rate law definition of general acid catalysis (*7*). Factors that may have contributed to a general acid pH−rate profile have been discussed (*13*, *18*), but of particular concern here was the possible role of trace divalent metal ion and the effect of high salt and low pH in reducing the association constant of EDTA for trace divalent metal ions. For the cleavage reactions in LiCl or NH_4Cl, increasing the EDTA concentration to 25 mM eliminated a small increase in rates at the lower pH values that were seen in 1 mM EDTA (data not shown). For reactions in NaCl, it was necessary to increase the EDTA concentrations to 0.1 M to suppress an increase in the rate at low pH. The higher (0.1 M) EDTA concentrations did not alter the cleavage rates in NaCl when the pH was ≥6, nor did it affect the rates in high concentrations of LiCl or NH_4Cl (data not shown). At pH values greater than ∼8.5, nonspecific RNA degradation

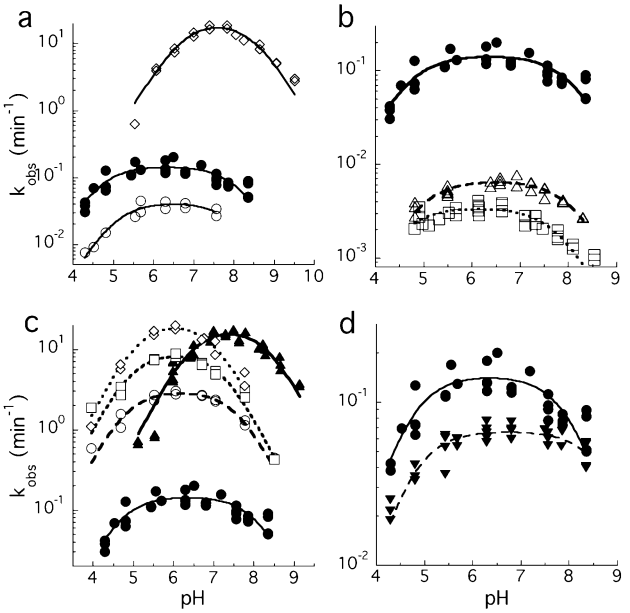

FIGURE 5: (a) pH−rate profiles in $MgCl_2$ and LiCl. Cleavage of the TGR1 genomic ribozyme in 11 mM $MgCl_2$ and 1 mM EDTA at 25 °C (◇) and in 4 M LiCl and 25 mM EDTA at 37 °C (●) or 25 °C (○). (b) pH−rate profiles (TGR1) in 4 M LiCl and 25 mM EDTA (●), 4 M NH_4Cl and 25 mM EDTA (△), and 4 M NaCl and 100 mM EDTA (□). All reactions were carried out at 37 °C. (c) pH−rate profiles (TGR1) at 37 °C in 4 M LiCl and 1 mM EDTA with increasing $MgCl_2$ concentrations [2, 3, and 6 mM (○, □, and ◇, respectively)] compared to pH−rate profiles in 2 mM $MgCl_2$ and 1 mM EDTA (▲) and 4 M LiCl and 25 mM EDTA (●). (d) Comparison of the pH−rate profile of the PEX1 antigenomic ribozyme (▽) to that of TGR1 in 4 M LiCl and 25 mM EDTA at 37 °C. Curves were generated by fitting data to the equation $k_{obs} = k_{max}/(1 + 10^{pK_{a1}-pH} + 10^{pH-pK_{a2}})$ using KaleidaGraph (Synergy Software).

in the monovalent salts interfered with quantification of ribozyme specific cleavage. As will also be noted below, it is likely that the true pH in 4 M monovalent salt is higher than what was actually measured. Thus, this degradation is likely to due to alkaline degradation of RNA which more typically seen above pH 9.5 or 10.

The appearance of a shifted pH optimum for the reactions in monovalent salt could have several possible explanations. Effects on the ionization of the buffer as well as on groups in the ribozyme are likely, but another source was the effect of high salt concentrations on proton activity measured with a glass electrode (*30*). The pH readings of strongly dissociating acid (HCl) and base (NaOH), with and without added salts, indicated that the pH readings at high salt concentrations are low by at least 1 pH unit (see Materials and Methods). As a test of this explanation for the shift, the pH−rate profiles for reactions with both 4 M LiCl and $MgCl_2$ were compared to those for reactions in just LiCl [4 M; Figure 5c (●)] or just $MgCl_2$ [1 mM (◆)]. All reactions were carried out at 37 °C, and the concentration of $MgCl_2$ was lowered to slow the reaction at this temperature [the pH−rate curve in 1 mM $MgCl_2$ at 37 °C (Figure 5c) was similar to the curve generated in 10 mM $MgCl_2$ at 25 °C (Figure 5a)]. For reaction mixtures containing both LiCl and $MgCl_2$, the EDTA concentration was reduced to 1 mM and $MgCl_2$ was added to a concentration of 2, 3, or 6 mM (approximately 1, 2, or 5 mM available Mg^{2+}, respectively) (Figure 5c, empty symbols). In these reactions, the pH optimum in just 4 M Li^+ was 6.4 ± 0.2, while in just 1 mM Mg^{2+}, it was 7.4 ± 0.2. In 4 M LiCl, the addition of 2 mM $MgCl_2$ stimulated activity 21-fold, 3 mM gave a 63-fold increase, and 6 mM gave a 153-fold increase. Rather than shifting the pH−rate profile toward the higher values seen for reactions in $MgCl_2$, the pH optimum for reactions in LiCl and $MgCl_2$ remained 1.2−1.5 units lower than in Mg^{2+} alone. The pH−rate profiles in 4 M LiCl and Mg^{2+} were bell-shaped with pH optima that were similar to each other (6.2 ± 0.2, 6.1 ± 0.2, and 5.9 ± 0.2, with 2, 3, and 6 mM $MgCl_2$, respectively) and only slightly lower than that seen in LiCl alone (Figure 5c). These data suggest that high concentrations of LiCl, not the absence of $MgCl_2$, caused the observed large difference in pH optima in the LiCl versus $MgCl_2$ reactions. That shift can be explained by a salt-dependent lowering of the pH reading by approximately 1 pH unit (see Materials and Methods), and we conclude that there is no large shift in the pH−rate curves when Mg^{2+} is omitted from the reaction.

For the antigenomic ribozyme, PEX1, the pH−rate dependence for cleavage of the reaction in LiCl could also be described as being bell-shaped, but it was broader than that seen with the genomic ribozyme [Figure 5d (▼)]. In 4 M LiCl, the antigenomic ribozyme has a k_{max} of 0.066 min^{-1} and apparent pK_a values of 4.7 and ∼8.8. An apparent pK_a in the high-pH range where deprotonation of guanine and uracil would be expected is also characteristic of the self-cleavage of the antigenomic ribozyme in Mg^{2+} (data not shown).

A difference in rates for reactions in LiCl and $MgCl_2$, at the optimal pH for the reaction in either salt, can be estimated from data presented here. In 5−10 mM $MgCl_2$, the reactions at 37 °C are too fast to measure accurately by hand (>20 min^{-1}), but with the Mg^{2+} concentration reduced to 1 mM, the reaction in $MgCl_2$ was still ∼100 times faster than in 4 M LiCl at 37 °C (Figure 5c). Similar increases were seen with the addition of 6 mM $MgCl_2$ to the reaction mixtures containing LiCl (Figure 5c). At 25 °C, the cleavage reaction in 10 mM Mg^{2+} was ∼500 times faster than the reaction in 4 M LiCl at 25 °C (Figure 5a). Thus, a minimum estimate for the contribution of Mg^{2+} to the cleavage rate would be in the range of 100−500-fold.

Cleavage Activity in Ammonium and Hydroxyammonium Ion. HDV ribozyme cleavage rates were slightly higher in NH_4Cl than in NaCl (Figures 2a,c and 3 and Table 1). We also found that the ribozymes were active in 0.1−2.0 M hydroxylamine at pH 5.8 (pK_a of hydroxylamine ∼ 6) (Figure 2d and data not shown). In 0.5 M NH_2OH, the rate of self-cleavage is ∼10-fold higher than in comparable concentrations of NH_4Cl (at pH 5.8), but the background rate of RNA degradation was also higher in NH_2OH than in NH_4Cl. The pH optimum for the NH_2OH reaction was near 6.2, and the pH−rate profile was bell-shaped and narrow (data not shown), suggesting that it may be the hydroxyammonium ion that supported the observed activity. The possibility that NH_2OH could have been acting as a general base catalyst or nucleophile in the cleavage reaction was not further investigated because of RNA degradation and instability of hydroxylamine at alkaline pH. As it stands, there are insufficient data to either support or definitively rule out a role for the non-metal cations as a general acid−base catalyst, but the data provide further support that a metal ion per se was not necessary for ribozyme cleavage.

Table 2: Thiophosphate Substitutions at the Scissile Phosphate Position[a]

	PEX1.2 (phosphate)		PEX1.2S (thiophosphate)		
	k_{obs}o	% cleaved[b]	k_{obs}s	k^O/k^{S} [c]	% cleaved[b]
10 mM $MgCl_2$ (pH 7.5)	$(3.1 \pm 0.9) \times 10$	7 ± 2	$(2.4 \pm 1.4) \times 10$	1.3	40 ± 3
4 M LiCl (pH 7.0)	$(3.6 \pm 0.3) \times 10^{-2}$	79 ± 2	$(2.6 \pm 0.2) \times 10^{-2}$	1.4	40 ± 2
4 M NH_4Cl (pH 6.8)	$(2.4 \pm 0.2) \times 10^{-3}$	85 ± 2	$(8.1 \pm 0.8) \times 10^{-2}$	1/34	40 ± 2
	TGR1.2 (phosphate)		TGR1.2S (thiophosphate)		
	k_{obs}o	% cleaved[b]	k_{obs}s	k^O/k^{S} [c]	% cleaved[b]
10 mM $MgCl_2$ (pH 7.5)	$(4.1 \pm 0.4) \times 10$	84 ± 4	$(3.6 \pm 0.6) \times 10$	1.1	37 ± 2
4 M LiCl (pH 6.8)	$(1.2 \pm 0.1) \times 10^{-1}$	88 ± 3	$(2.3 \pm 0.6) \times 10^{-2}$	5.2	39 ± 2
4 M NH_4Cl (pH 6.6)	$(7.8 \pm 0.3) \times 10^{-3}$	76 ± 4	$(1.4 \pm 0.1) \times 10^{-1}$	1/18	37 ± 1
4 M NaCl (pH 6.5)	$(2.6 \pm 0.2) \times 10^{-3}$	86 ± 3	$(8.6 \pm 0.7) \times 10^{-3}$	1/3.3	42 ± 1
1 M NH_2OH (pH 5.6)	$(2.0 \pm 0.3) \times 10^{-2}$	73 ± 3	$(1.9 \pm 0.4) \times 10^{-2}$	1/1.1	24 ± 2

[a] All rate constants (k_{obs}) have units of inverse minutes. [b] The % cleaved is the extent of reaction. [c] k^O/k^S is the thio effect, the ratio of cleavage rate constants for the phosphate over the thiophosphate.

Thiophosphate Substitutions at the Cleavage Site. Thiophosphate substitutions can be used both as a probe for potential metal ion coordination and to slow the reaction chemistry. Previous studies revealed that the pro-R_P oxygen to sulfur substitution strongly inhibits cleavage of the HDV ribozyme in Mg^{2+} (*31*), and there was no evidence that activity could be rescued with the addition of a more thiophilic metal ion such as Mn^{2+} or Cd^{2+}. With the pro-S_P substitution, the rate of cleavage in Mg^{2+} was not greatly affected (*31*). Here, the effect of thiophosphate substitutions on cleavage in monovalent cations was compared to those results. Antigenomic ribozymes with a single thiophosphate at the cleavage site were constructed by ligation of synthetic oligoribonucleotides to the 5′ end of a truncated ribozyme. A control, all-phosphate, ribozyme was similarly constructed. These constructs (PEX1.2 and PEX1.2S for phosphate and thiophosphate, respectively) were tested for self-cleavage in the various cations (Table 2). For reactions in 10 mM Mg^{2+}, the phosphate and thiophosphate ribozymes cleaved with rate constants in excess of 10 min^{-1} (measured manually). While the phosphate possibly cleaved faster, the rate constants were too fast to measure accurately. However, the extent of the reaction for PEX1.2S was half that of the phosphate version. Since PEX1.2S was a mixed diastereoisomer, those results are consistent with previously reported findings that the S_P isomer was preferentially cleaved (*31*). Inhibition of cleavage in $MgCl_2$ by the R_P configuration at the cleavage site was also consistent with our data from ribozymes transcribed with [α-thio]-NTPs (unpublished data). For reactions in 4 M LiCl, the thiophosphate modification resulted in both a small decrease in the rate of cleavage (from 0.036 to 0.026 min^{-1}) and a 2-fold decrease in the extent of cleavage (from 79 to 40%) (Table 2). Metal ion mixing experiments indicated that the same population of the thiophosphate-containing ribozyme was being cleaved in both LiCl and $MgCl_2$. For those experiments, $MgCl_2$ and LiCl were added either concurrently or sequentially, and in no case was there an increase in the extent of cleavage of the thiophosphate-containing ribozyme (data not shown). In that the ribozyme fraction that cleaved in Mg^{2+} has previously been determined to be the S_P isomer (*31*), we conclude that substitution of the pro-R_P oxygen strongly inhibits cleavage regardless of the cation, whereas substitution of the pro-S_P oxygen had a small effect on the rate.

There was, however, with respect to the rates of cleavage, an unexpected inverse thio effect (k^o/k^s) for the reaction in NH_4Cl. The extent of reaction decreased from 85 to 40% for the thiophosphate (Table 2), consistent with cleavage of only the S_P diastereoisomer of PEX1.2S. However, the cleavage rate constant for the thiophosphate (k_{obs}s) increased ~34-fold relative to that of the phosphate (k_{obs}o, from 0.0024 to 0.081 min^{-1}) (Table 2). A small inverse thio effect (1.4−1.8-fold) has be found previously for cleavage of an S_P-thiophosphate linkage by the hairpin ribozyme (*15*). The data here suggest that that effect can be quite large. In addition, the cleavage rate for the thiophosphate ribozyme in NH_4Cl was faster than the phosphate version (PEX1.2 or PEX1) in LiCl. Unless the mechanism of catalysis for cleavage of the thiophosphate and phosphate forms were different, the chemistry for cleavage of the thiophosphate form would be slower, not faster, than the phosphate form (*32*, *33*). If there had been no thio effect, one interpretation would be that a nonchemistry step, possibly a conformational change, was rate-determining for both the phosphate and thiophosphate. A large inverse thio effect appears to be more difficult to explain, but it is possible that in NH_4^+, the active site geometry with the thiophosphate was more favorable for cleavage than with the phosphate. As a result, cleavage chemistry at the phosphate may be slower because the participating groups are suboptimally positioned, or cleavage may require a slower conformational change to correct that positioning prior to chemistry.

The inverse thio effect was not limited to the antigenomic form of the ribozyme. A thiophosphate version of the genomic form of the ribozyme (TGR1.2 and TGR1.2S) gave similar results (Table 2). For reactions in Mg^{2+}, there was a small decrease in the k_{obs}s and the extent of reaction decreased by more than half. With all of the monovalent cations that were tested, the extent of the reaction was likewise reduced for the thiophosphate. There was consistently a larger decrease in the extent of cleavage for TGR1.2S, relative to that for TGR1.2, compared to what was seen with PEX1.2S and PEX1.2. This difference was attributed to the 10−15% cleavage that occurred during the ligation reaction used in preparations of the precursor form of the genomic ribozyme which would partially deplete the more reactive diastereoisomer prior to isolation of the precursors. In 4 M LiCl, k_{obs}s was decreased 5-fold relative

to k_{obs}o. This thio effect was larger than that seen with the antigenomic ribozyme. However, the two thiophosphate-containing ribozymes (TGR1.2S and PEX1.2S) were cleaved with similar rate constants in LiCl. The larger thio effect with the genomic ribozyme was thus attributed to the higher rate of cleavage of TGR1.2 in LiCl, and together, the data are consistent with chemistry being rate-determining for cleavage of the thiophosphate-containing ribozymes in LiCl, as well as for TGR1.2. In 4 M NH_4Cl, the thiophosphate cleaved 18-fold faster than did the phosphate form. Thus, as with the antigenomic ribozyme, there was an inverse thio effect for the reactions in NH_4Cl. A small inverse thio effect in 4 M NaCl was also seen, with TGR1.2S cleaving 3-fold faster than TGR1.2.

These results argue that, depending on the cation, different rates for the ribozyme cleavage reactions could reflect different rate-determining steps. Only in LiCl, where the reaction was fastest, did cleavage of TGR1.2 and TGR1.2S ribozymes show a significant thio effect that would be consistent with chemistry being rate-limiting. The thio effect with PEX1.2 and PEX1.2S in LiCl was smaller, but the PEX1.2S was cleaving at approximately the same rate as the TGR1.2S, again suggesting that chemistry is rate-determining in LiCl.

The Active Site Cytosine Is Required for Cleavage in Monovalent Salts. Structural and biochemical evidence suggests a catalytic role for the cytosine at position 75 (C75) in the genomic ribozyme (C76 in the antigenomic ribozyme) (*4*, *7*−*9*, *12*). For reactions in Mg^{2+}, changing the C to an A reduced activity 10^3-fold, and deleting the C or changing it to G or U reduced cleavage rates further. However, activity in $MgCl_2$ could be partially rescued with free cytosine base or imidazole buffer (*8*, *9*). Cleavage activity of the C75a and C75u genomic ribozyme mutants in 4 M LiCl was examined, and with either mutation, the cleavage activity was reduced to near-uncatalyzed rates ($\leq 10^{-5}$ min^{-1} at neutral pH). A small amount (~1%) of product-size RNA was generated with the C75u mutant after 24 h at 37 °C (data not shown), but that reaction was not further characterized. No cleavage product was observed for C75a under similar conditions. Finally, there was no detectable rescue of activity of the C75 mutants when cytosine or imidazole was added to the reaction mixture, and similar results were obtained with the antigenomic C76 mutant ribozyme in LiCl (data not shown). It appears that self-cleavage activity in LiCl is strongly dependent on the cytosine at position 75 (*76*). The interesting exception was the slight activity of the C75/76u mutants.

DISCUSSION

We have examined and compared the activity of the two HDV ribozymes in various monovalent salts. In the absence of added divalent metal ions, self-cleaving forms of both HDV ribozymes were active in high concentrations of monovalent salts. The reactions were nearly 50 times faster in LiCl than in NaCl or NH_4Cl. For reactions in LiCl, the data suggested that chemistry was rate-determining, whereas the slower reactions in NaCl or NH_4Cl displayed an unusual inverse thio effect. LiCl also supported the highest cleavage rates of the hammerhead ribozyme in monovalent salts (*20*, *21*). It is possible that Li^+ is more effective than Na^+ in the stabilization structure of the ribozyme, but given the smaller size and higher charge density of Li^+ relative to Na^+, it is also possible that the high Li^+ concentration is better able to partially substitute in the catalytic role of lower concentrations of Mg^{2+}. The cleavage rates in LiCl were still 2−3 orders of magnitude slower than those when Mg^{2+} was available, and despite the decrease in the rate of cleavage, the shape of the pH−rate profile for the reactions was not dramatically changed for reactions in LiCl compared to those in $MgCl_2$. The similarity of pH−rate profiles was most evident when $MgCl_2$ is added back to reaction mixtures containing LiCl since this prevented an artifactual pH shift.

The results of these studies support the hypothesis that, while the HDV ribozymes are active in the absence of divalent metal ions if provided high concentrations of monovalent cations, higher rates are greatly facilitated by Mg^{2+}. Thus, in the broad definition, Mg^{2+} was acting as a catalyst. However, it is useful to distinguish between rate enhancement due to the metal ion-stabilizing RNA structure and a metal ion acting as a catalytic group. Nakano et al. (*13*, *34*) determined that for the HDV genomic ribozyme reactions in NaCl and $MgCl_2$, there were both structural and catalytic contributions by Mg^{2+}, and the larger contribution was structural. They used a form of the genomic ribozyme different from that used here, and it cleaves slower; therefore, the results from the two labs may not be strictly comparable. Nevertheless, it is likely that the finding of both structural and catalytic contributions by the Mg^{2+} would be generally true for the HDV ribozymes, even at the higher LiCl concentration that we used to support activity.

The inhibition of the Mg^{2+} reaction by monovalent salts was also suggestive of a catalytic role for divalent metal ion, be it directly as a metal ion catalyst or indirectly through a structural effect. LiCl inhibited the Mg^{2+}-dependent reaction, but with a higher $MgCl_2$ concentration, a ribozyme·Li^+·Mg^{2+} complex cleaved with rates similar to those of the ribozyme·Mg^{2+} complex. Inhibition of Mg^{2+}-dependent cleavage by LiCl shows characteristics of competitive partial inhibition where binding of Li^+ increases the apparent K_d for a catalytic Mg^{2+} but will not totally suppress the Mg^{2+}-dependent reaction. It was curious that high LiCl concentrations failed to reduce activity to the rate of the LiCl-only reactions, but a similar, and more dramatic, effect was seen with the hammerhead ribozyme where the effect of mixing monovalent and divalent metal ions has been examined in detail (*22*). Two contrasting effects of monovalent salt on the Mg^{2+} reaction were observed with the hammerhead ribozyme. First, there was a partial decrease in Mg^{2+}-dependent activity with an increase in NaCl concentration (to ~1 M), but that was followed by a return to the faster rate at very high NaCl concentrations (3−4 M). Thus, the NaCl acted as an inhibitor at low concentrations (<1 M), but not at higher concentrations. An interpretation of that data was that Na^+, at the lower concentration, competes with Mg^{2+} binding, but at higher concentrations, Na^+ stabilizes the structure and a binding site that prefers Mg^{2+}. It is possible that, in the HDV ribozymes, monovalent metals have a similar effect in stabilizing divalent metal ion binding at some sites while also competing for other binding sites. This interpretation could explain why the cleavage rates at high LiCl concentrations with low $MgCl_2$ concentrations remain faster than those in LiCl alone. It might also help explain the observation that

EDTA, especially at low pH, appears to be a particularly poor competitive chelator of divalent metal ion in ribozyme reaction mixtures containing high NaCl concentrations (*18*).

The pH−rate profile for the genomic HDV ribozyme is a bell-shaped curve, suggesting that there are probably two ionizable groups with pK_a values within the experimental range that limit the cleavage rates. This bell-shaped profile is not fully explained from models for catalytic mechanisms currently proposed for the HDV ribozymes (*6*, *7*) because the only proposed ionizable group with a pK_a in the experimental pH range is C75 (C76). One possibility consistent with the mechanism is that a second nucleobase, with an ionization constant close to the neutral range, affects cleavage rates indirectly through its effect on structure or an influence of its charge on catalysis and, thus, contributes to the second leg of the bell-shaped curve. In the genomic ribozyme, a candidate for this nucleobase is C41, which is involved in a base quadruple (*4*, *5*). The base quadruple may contribute to catalysis because it provides part of a "pedestal" for the active site and could stabilize or alter transition state geometry. The same quadruple arrangement is found in a frame-shifting pseudoknot studied by NMR, and those data indicate that the cytosine is protonated (*35*, *36*). In support of the idea that a protonated C41 contributes to stability, activity, and the shape of the pH−rate profile of the genomic ribozyme in monovalent salts, we note that the antigenomic ribozyme lacks the sequence that would form this feature and it was less stable (*18*), required higher concentrations of monovalent salts to stimulate cleavage activity, and had a broader pH−rate profile.

The absence of an inversion in the shape of the pH−rate profiles for the genomic ribozyme reaction with and without Mg^{2+} was at odds with some of the data supporting a particular model of the catalytic mechanism of the ribozymes (*7*). However, if one argued that the model does not necessarily predict a pH−rate curve inversion in the absence of Mg^{2+}, then this newer data cannot rule out the model either. A decrease in cleavage rates seen in 1 M NaCl relative to reactions in $MgCl_2$, which was accompanied by an inversion of the pH−rate profile (from a general base to general acid pH−rate profile), was provided as evidence of a role for $Mg(OH)^+$ as a general base catalyst (*7*). In an attractive model of a concerted general acid−base mechanism in the genomic ribozyme, the $Mg(OH)^+$ accepts the proton from the 2′-OH group, while the protonated active site cytosine (C75-H^+) donates a proton to the 5′-OH leaving group oxygen (Figure 6). An active site cytosine (C75) was proposed by Ferré-D'Amaré et al. (*4*) from their structure, and it was suggested that the cytosine could be acting as a general acid−base catalyst, but at the 2′-hydroxyl. Chemical rescue experiments in the antigenomic and genomic HDV ribozymes (*8*, *9*, *11*) provide evidence that the active site cytosine acts as a general acid−base catalyst, but those data do not distinguish between two likely sites of action in the cleavage reaction, the 2′-OH group or the 5′-bridging oxygen. The inversion of the pH−rate profile appeared to resolve the ambiguity, but then it was found that the shape of the pH−rate profile for the reaction in NaCl may also reflect the ionization of groups other than the active site cytosine (*18*). Of particular concern was the relative affinities of EDTA and the ribozyme for Mg^{2+} at high salt concentrations and low pH; it turned out that higher concentrations (25−100 mM) of EDTA were required to effectively chelate divalent metal ions at the lower pHs (*13*, *18*). Also complicating the meaning of the pH−rate data for the genomic ribozyme was the base quadruple, mentioned earlier, that contains an ionizable base (C41) (*5*). C41, or another component of the base quadruple, was not hypothesized to have a direct catalytic role, but ionization appeared to alter the stability of the ribozyme in 1 M NaCl and enhance activity in NaCl (*18*). Despite these issues, the model for C75 acting as a general acid catalyst in the cleavage reaction remains attractive and recently received strong support from biochemical data that convincingly point to its involvement in facilitating proton transfer to the 5′-bridging oxygen of the scissile phosphate to make it a better leaving group in the cleavage reaction (*12*). A favored model for the role of Mg^{2+} thus may continue to be one in which it acts as a partial proton acceptor (general base) to activate the 2′-OH group. However, given the similarity in pH−rate profiles for the reactions with and without Mg^{2+}, additional approaches and experiments that will strengthen support for a specific role of the Mg^{2+} in catalysis are necessary.

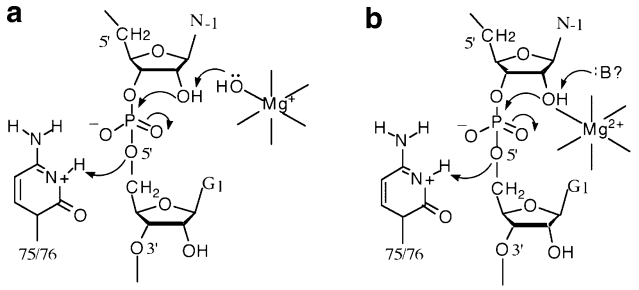

FIGURE 6: Possible roles for catalytic groups. (a) Concerted general base−acid-catalyzed cleavage in the HDV ribozymes. A protonated cytosine (C75/C76) acts as a proton donor, and a hydroxide ion bound to Mg^{2+} acts as a proton acceptor. (b) An alternative model in which the metal ion binds directly to the 2′-oxygen to stabilize the loss of the proton from that position. Not shown is a possible additional need for an electrostatic catalyst to shield charge that develops on the phosphate; this might be provided by either a metal ion or a nucleobase.

ACKNOWLEDGMENT

We thank A. Brown and S. Wilkinson for reading earlier versions of the manuscript.

REFERENCES

1. Branch, A. D., and Robertson, H. D. (1984) A replication cycle for viroids and other small infectious RNA's, *Science 223*, 450−455.
2. Robertson, H. D. (1992) Replication and evolution of viroid-like pathogens, *Curr. Top. Microbiol. Immunol. 176*, 213−219.
3. McKay, D. B., and Wedekind, J. E. (1998) in *The RNA World* (Gesteland, R. F., Cech, T. R., and Atkins, J. F., Eds.) pp 265, Cold Spring Harbor Laboratory Press, Plainview, NY.
4. Ferré-D'Amaré, A. R., Zhou, K., and Doudna, J. A. (1998) Crystal structure of a hepatitis delta virus ribozyme, *Nature 395*, 567−574.
5. Ferré-D'Amaré, A. R., and Doudna, J. A. (2000) Crystallization and structure determination of a hepatitis delta virus ribozyme: Use of the RNA-binding protein U1A as a crystallization module, *J. Mol. Biol. 295*, 541−556.
6. Ke, A., Zhou, K., Ding, F., Cate, J. H., and Doudna, J. A. (2004) A conformational switch controls hepatitis delta virus ribozyme catalysis, *Nature 429*, 201−205.
7. Nakano, S.-I., Chadalavada, D. M., and Bevilacqua, P. C. (2000) General acid-base catalysis in the mechanism of a hepatitis delta virus ribozyme, *Science 287*, 1493−1497.

8. Perrotta, A. T., Shih, I.-h., and Been, M. D. (1999) Imidazole Rescue of a Cytosine Mutation in a Self-Cleaving Ribozyme, *Science 286*, 123−126.
9. Shih, I.-h., and Been, M. D. (2001) Involvement of a cytosine side chain in proton transfer in the rate-determining step of ribozyme self-cleavage, *Proc. Natl. Acad. Sci. U.S.A. 98*, 1489−1494.
10. Shih, I.-h., and Been, M. D. (2002) Catalytic strategies of the hepatitis delta virus ribozymes, *Annu. Rev. Biochem. 71*, 887−917.
11. Perrotta, A. T., Wadkins, T. S., and Been, M. D. (2006) Chemical rescue, multiple ionizable groups, and general acid−base catalysis in the HDV genomic ribozyme, *RNA 12*, 1282−1291.
12. Das, S. R., and Piccirilli, J. A. (2005) General acid catalysis by the hepatitis delta virus ribozyme, *Nat. Chem. Biol. 1*, 45−52.
13. Nakano, S.-I., Proctor, D. J., and Bevilacqua, P. C. (2001) Mechanistic characterization of the HDV genomic ribozyme: Assessing the catalytic and structural contributions of divalent metal ions within a multi-channel reaction mechanism, *Biochemistry 40*, 12022−12038.
14. Hampel, A., and Cowan, J. A. (1997) A unique mechanism for RNA catalysis: The role of metal cofactors in hairpin ribozyme cleavage, *Chem. Biol. 4*, 513−517.
15. Nesbitt, S., Hegg, L. A., and Fedor, M. J. (1997) An unusual pH-independent and metal-ion-independent mechanism for hairpin ribozyme catalysis, *Chem. Biol. 4*, 619−630.
16. Young, K. J., Gill, F., and Grasby, J. A. (1997) Metal ions play a passive role in the hairpin ribozyme catalysed reaction, *Nucleic Acids Res. 25*, 3760−3766.
17. Murray, J. B., Seyhan, A. A., Walter, N. G., Burke, J. M., and Scott, W. G. (1998) The hammerhead, hairpin and VS ribozymes are catalytically proficient in monovalent cations alone, *Chem. Biol. 5*, 587−595.
18. Wadkins, T. S., Shih, I., Perrotta, A. T., and Been, M. D. (2001) A pH-sensitive RNA tertiary interaction affects self-cleavage activity of the HDV ribozymes in the absence of added divalent metal ion, *J. Mol. Biol. 305*, 1045−1055.
19. Roth, A., Nahvi, A., Lee, M., Jona, I., and Breaker, R. R. (2006) Characteristics of the glmS ribozyme suggest only structural roles for divalent metal ions, *RNA 12*, 607−619.
20. O'Rear, J. L., Wang, S., Feig, A. L., Beigelman, L., Uhlenbeck, O. C., and Herschlag, D. (2001) Comparison of the hammerhead cleavage reactions stimulated by monovalent and divalent cations, *RNA 7*, 537−545.
21. Curtis, E. A., and Bartel, D. P. (2001) The hammerhead cleavage reaction in monovalent cations, *RNA 7*, 546−552.
22. Zhou, J. M., Zhou, D. M., Takagi, Y., Kasai, Y., Inoue, A., Baba, T., and Taira, K. (2002) Existence of efficient divalent metal ion-catalyzed and inefficient divalent metal ion-independent channels in reactions catalyzed by a hammerhead ribozyme, *Nucleic Acids Res. 30*, 2374−2382.
23. Perrotta, A. T., and Been, M. D. (1990) The self-cleaving domain from the genomic RNA of hepatitis delta virus: Sequence requirements and the effects of denaturant, *Nucleic Acids Res. 18*, 6821−6827.
24. Wadkins, T. S., and Been, M. D. (1997) Core-associated non-duplex sequences distinguishing the genomic and antigenomic self-cleaving RNAs of hepatitis delta virus, *Nucleic Acids Res. 25*, 4085−4092.
25. Perrotta, A. T., and Been, M. D. (1998) A toggle duplex in hepatitis delta virus self-cleaving RNA that stabilizes an inactive and a salt-dependent pro-active ribozyme conformation, *J. Mol. Biol. 279*, 361−373.
26. Ellis, K. J., and Morrison, J. F. (1982) Buffers of constant ionic strength for studying pH-dependent processes, *Methods Enzymol. 87*, 405−426.
27. Perrotta, A. T., Nikiforova, O., and Been, M. D. (1999) A conserved bulged adenosine in a peripheral duplex of the antigenomic HDV self-cleaving RNA reduceskinetic trapping of inactive conformations, *Nucleic Acids Res. 27*, 795−802.
28. Moore, M. J., and Sharp, P. A. (1992) Site-Specific Modification of Pre-mRNA: The 2′-Hydroxyl Groups at the Splice Sites, *Science 256*, 992−997.
29. Shih, I.-h., and Been, M. D. (1999) Ribozyme cleavage of a 2′,5′-phosphodiester linkage: Mechanism and a restricted divalent metal ion requirement, *RNA 5*, 1140−1148.
30. Bostrom, M., Craig, V. S. J., Albion, R., Williams, D. R. M., and Ninham, B. W. (2003) Hofmeister Effects in pH Measurements: Role of Added Salt and Co-Ions, *J. Phys. Chem. B 107*, 2875−2878.
31. Jeoung, Y.-H., Kumar, P. K. R., Suh, Y.-A., Taira, K., and Nishikawa, S. (1994) Identification of phosphate oxygens that are important for self-cleavage activity of the HDV ribozyme by phosphorothioate substitution interference analysis, *Nucleic Acids Res. 22*, 3722−3727.
32. Herschlag, D., Piccirilli, J. A., and Cech, T. R. (1991) Ribozyme-catalyzed and nonenzymatic reactions of phosphate diesters: Rate effects upon substitution of sulfur for a nonbridging phosphoryl oxygen atom, *Biochemistry 30*, 4844−4854.
33. Herschlag, D. (1994) Ribonuclease Revisited: Catalysis via the Classical General Acid-Base Mechanism or Triester-like Mechanism, *J. Am. Chem. Soc. 116*, 11631−11635.
34. Nakano, S., Cerrone, A. L., and Bevilacqua, P. C. (2003) Mechanistic characterization of the HDV genomic ribozyme: Classifying the catalytic and structural metal ion sites within a multichannel reaction mechanism, *Biochemistry 42*, 2982−2994.
35. Nixon, P. L., and Giedroc, D. P. (2000) Energetics of a strongly pH dependent RNA tertiary structure in a frameshifting pseudoknot, *J. Mol. Biol. 296*, 659−671.
36. Nixon, P. L., Rangan, A., Kim, Y. G., Rich, A., Hoffman, D. W., Hennig, M., and Giedroc, D. P. (2002) Solution structure of a luteoviral P1-P2 frameshifting mRNA pseudoknot, *J. Mol. Biol. 322*, 621−633.

BI061215+